Experimental Study on Detonation Propagation in Annular Channels

Jian LI*, Shun-jiang HE
State Key Laboratory of Explosion Science and Technology, Beijing Institute of Technology
Beijing, China

1 Introduction

The continuous rotary detonation engine (CRDE) has many advantages, such as high specific impulse, stable thrust, compact structure, etc. In recent years, the propagation characteristics of the detonation wave in the combustor and pipe of CRDE have caused extensive research [1-2]. A pre-detonation tube is usually used to initiate the detonation. One end of the pre-detonation tube is tangentially connected to the annular combustion chamber, and the other is connected with a spark plug. The detonation wave in the pre-detonation tube enters the main combustor and finally initiates the gas in the combustor after a series of complex and transient reflection processes. [3-4]

When a plane detonation wave enters a curved channel from a straight pipe, the inner side of the wavefront is diffracted, and thus the velocity is reduced, resulting in a wider reaction zone and enlarged cells. If the expansion is strong, the leading shock may be decoupled from the reaction zone, causing the failure of the detonation wave locally [5-6]. In contrast, the detonation on the outside of the curved pipe accelerates to an overdriven wave because of the Mach reflection. When the triple-point of the Mach reflection meets with the head of the expansion wave, these two processes begin to affect each other, which is a reasonably complicated process related to the geometry of the channel and the characteristic length of the detonation itself [7-14].

To understand the propagation mechanism of the detonation wave from the pre-detonation tube into the annular channel, in this abstract, by using the high-speed photography technology and multi-frame short-time open shutter camera method, the propagation processes of detonation waves in the annular channel were experimentally studied and analyzed. We focuses on the potential influence of channel width and cell size on the establishment of the detonation wave in the annular channel through the details of wave structure evolution and detonation limits, hoping to provide a reference for the design of the ignitor of CRDE.

2 Experimental setup

As shown in Fig.1(a), the experimental apparatus consists of a 1.5-m long, 3-cm diameter circular steel pre-detonation tube connected at the center with a cylindrical detonation chamber. The two cylindrical detonation chamber consists of two 1-m diameter circular plates, one steel

Correspondence to: jian_li@bit.edu.cn

and one glass, spaced by an o-ring, resulting in a cylindrical chamber of 10-cm thickness. The Schelkin spiral was inserted into the pre-detonation tube to accelerate the formation of detonation. Fig.1(b) shows a schematic diagram of the annular channel hollowed out of a PTFE plate of 10 mm thickness, which is then inserted into the cylindrical chamber clamped by the two parallel plates. The flatness and roughness of the PTFE plate are strictly guaranteed to ensure the sealing. The outer radius of the annular channel R is fixed as 136.5 mm, but the inner radius is changed such as to control the channel width w, that is, $w = R - R_n$. Four different channel widths w were considered: 30 mm, 50 mm, 70 mm, and 90 mm. To ensure that a stable CJ detonation wave can be formed before entering the annular channel, a U-shaped pipe of the width D =30 mm was used to connect the annular channel and the pre-detonation tube. Unstable C_2H_2+2.5O_2 mixtures, stable C_2H_2+2.5O_2+40%Ar and C_2H_2+2.5O_2+70%Ar were used in the experiment.

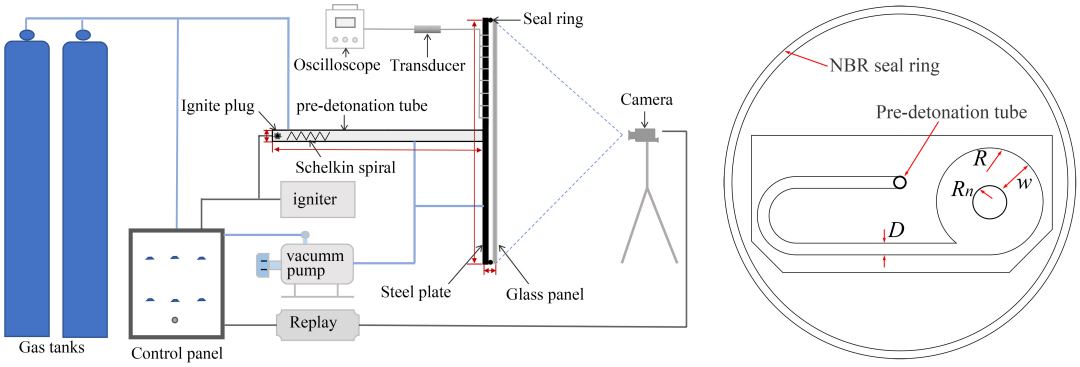

(a) (b)

Fig.1 Schematic diagram of the detonation experimental setup

The high-speed photography technology was used to collect the details of the detonation wave in the annular channel, particularly the triple-wave point trajectories in the entire channel, by using the so-called Multi-frame short-time open-shutter photography (MSOP) [15]. Fig.2(a) shows multi frames of short-time open-shutter photography, which were then superimposed together as the final result, as shown in Fig.2(b).

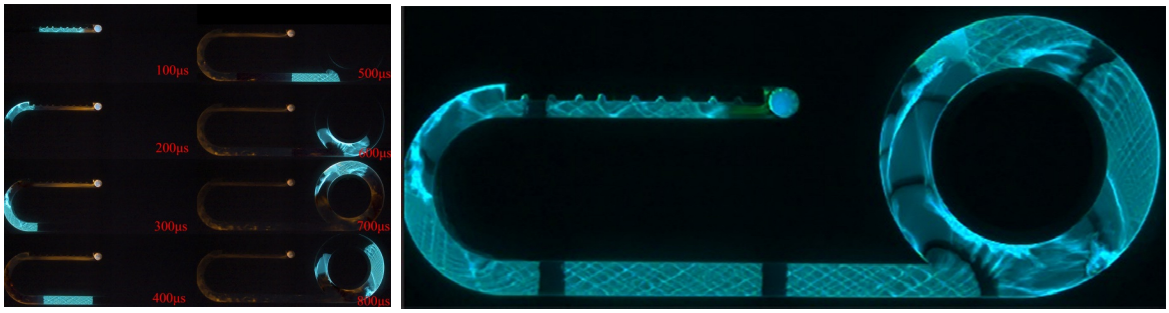

(a) single frames (b) superimposed frames

Fig.2 High-speed photographic images and MSOP processing image

3 Results and discussions

2.1 Propagation modes

The present study is similar to the classical problem of detonation diffraction into free space. However, in the current abstract, the free space becomes an annular channel, and the failure and re-initiation of the detonation are strongly affected by the boundary conditions. According to the classical problem of detonation diffraction, the propagation mode can be divided into three modes, i.e., subcritical, critical, and supercritical. However, in the present study, the detonations propagate clockwise and counterclockwise simultaneously when entering the annular channel, rendering different modes.

When the initial pressure is as low as 0.83 kPa, the detonations in the annular channel behave as a subcritical mode, as shown in Fig.3. In the straight pipe, a stable CJ detonation wave is generated and then enters the annular channel along the tangential direction. The detonation wave diffraction occurs due to the sudden increase in the flow area. It can be observed that the detonation waves decouple and fail quickly, forming a high-speed flame, and the flame front near the inner wall is far ahead of that near the outer wall. The detonation wave propagating counterclockwise can maintain a certain distance of cellular structure through the collision of the shear waves and the compression of the outer wall, but it finally fails. Due to local shock-frame interaction at the top of the channel, re-initiation may occur with extremely fine cells, as shown in Fig.3(c).

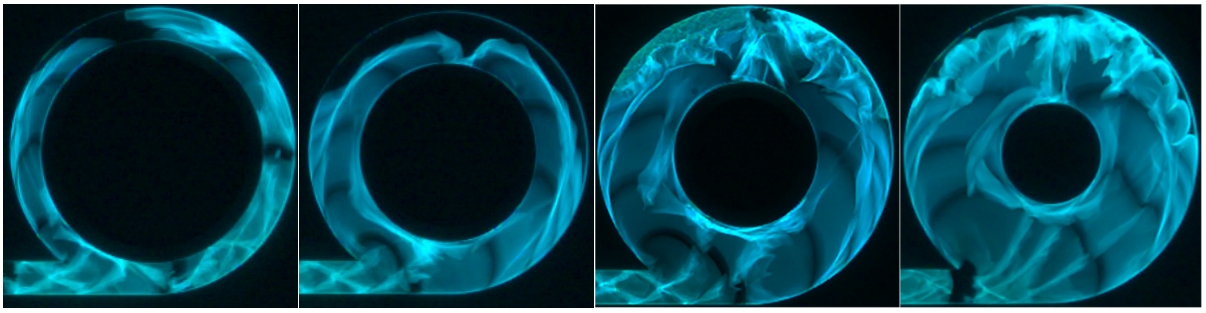

(a) w = 30 mm (b) w = 50 mm (c) w = 70 mm (d) w = 90 mm

Fig.3 MSOP images of C_2H_2+2.5O_2 at an initial pressure of 0.83 kPa

shown in Fig.4(a), when w = 30 mm, p = 1.6 kPa, the entire wavefront decouples completely. However, the decoupled wavefront collides with the inner wall, and regular and Mach reflections occur soon afterward. The intensity of the reflection depends on the angle of incidence. The reflection to the left is weaker, and the decoupled wavefront cannot be re-initiated. The reflection to the right is more vital, forming a strong transverse detonation wave to re-initiate the decoupled front. The transverse detonation wave reflects on the outer wall of the annular channel, initiating a second transverse detonation, which eventually evolves into a coupled and stable detonation wave. When the channel width is increased to 50 mm, as shown in Fig.4(b), the cellular pattern in the annular channel is the same as in Fig.4(a). The only difference is that the detonation wave counterclockwise is re-initiated with only one transverse detonation in Fig.4(b). As the channel width increased to 70 mm, as shown in Fig.4(c), the decoupled detonation wave cannot be re-initiated through reflection on the inner wall. This is because the increase in the width of the channel increases the distance at which the decoupled detonation wave decays, which enhances the attenuation. Thus the reflection on the inner wall is not strong enough to re-initiate. However, the high-speed flame counterclockwise due to continuous compression results in a local DDT process to realize the detonation reinitiation. In Fig.4(d), w = 90 mm, the detonation wave propagation mode is basically the same as the case with w = 70 mm.

If the initial pressure is further increased, the detonation wave propagating counterclockwise is in supercritical mode, as shown in Fig.5. For the propagation clockwise, two different modes arise; the first one, as shown in Fig.5(a), the reflection on the inner wall surface causing a re-initiation, and the second one as shown in Fig.5(b)-(d), the re-initiation is achieved by the transverse detonation wave rather than the reflection on the inner wall. Compared with Fig.4, it can be observed that in the supercritical mode, although the local front is briefly extinguished due to diffraction, the initial pressure is large enough to overcome the diffraction effect. On the left and right sides of the annular channel, the detonation cells are tiny, and the shock wave and reaction area have never been decoupled, which is due to the balance between the reduction effect of the expansion wave of the inner wall and the compression

enhancement of the outer wall. Compared with results at low initial pressures, the wave surface is smooth and exhibits significant bending caused by the geometry of the annular channel.

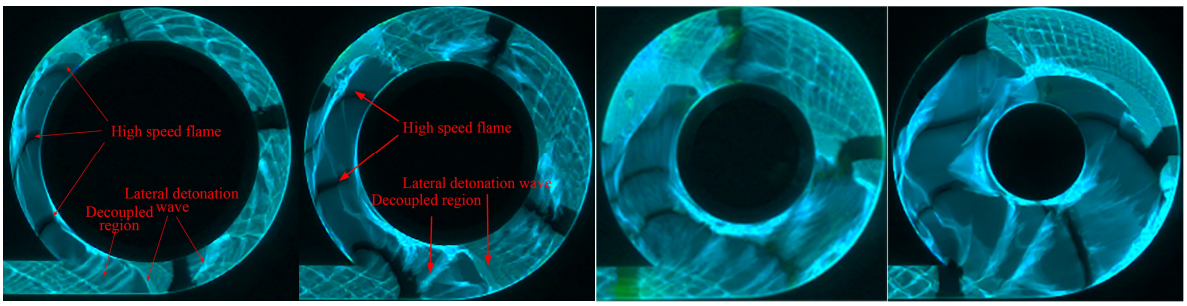

(a) w = 30 mm (b) w = 50 mm (c) w = 70 mm (d) w = 90 mm

Fig.4 MSOP images of C_2H_2+2.5O_2 at an initial pressure of 1.6 kPa

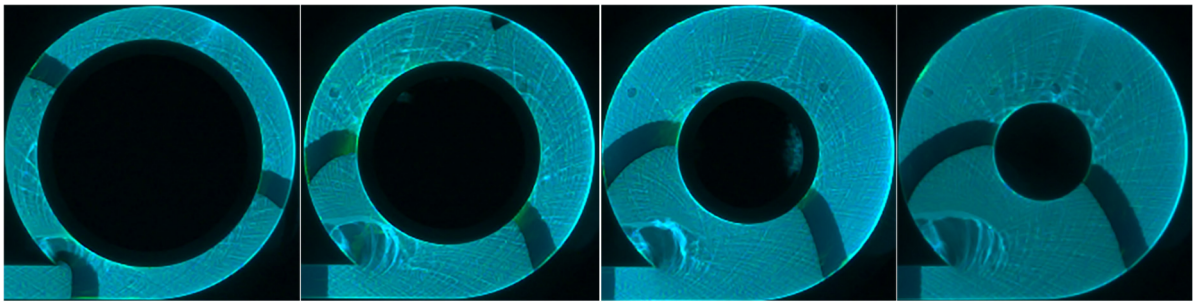

(a) w = 30 mm, p = 3.45 kPa (b) w = 50 mm, p = 3.45 kPa (c) w = 136.5 mm, p = 3.45 kPa (d) w = 90 mm, p = 3.45 kPa

Fig.5 MSOP images of C_2H_2+2.5O_2 gas in supercritical mode

2.2 Detonation limit and critical pipe diameter

For general hydrocarbon fuel mixtures, for the three-dimensional cases of detonation diffraction, many studies have confirmed the universal applicability of the empirical formula of critical tube diameter, $D_c \approx 13\lambda$ [16]. But many studies have also found that $D_c \approx 25\lambda$ for mixtures diluted with argon and $D_c \approx 13\lambda$ for unstable mixtures still hold. For two-dimensional cases, for stable gases, the critical tube width $D_c \approx 13\lambda$, and for unstable gases $D_c \approx 5\lambda$, the relevant studies can refer to the literature [17-18].

Figure 6 shows the detonation limits in clockwise (CW) and counterclockwise (CCW) directions. As shown in Fig.6(a), the critical pressure in the counterclockwise direction is smaller than that in the clockwise direction. Meanwhile, the critical pressure in the clockwise direction is basically unchanged with the increase in the channel width. However, the critical pressure in the counterclockwise direction increases with the channel width and eventually approaches a constant value. The critical pressure of unstable mixtures is smaller than that of stable mixtures. The critical pressure is converted into a dimensionless critical tube width D/λ (the straight tube), as shown in Fig.6(b). It is found that with the increase in the channel width w, for both stable and unstable detonations, the critical tube width D/λ is close to which is consistent with the critical tube diameter of the unstable detonation in the classical diffraction problem. If the channel width w is small, the detonation limit in the counterclockwise direction is less than 5, while in the clockwise direction, the value is basically close to 5. Even though inevitable fluctuations exist in the measurement of cell sizes, the range is almost limited to a cell size. Thus, it can be basically considered that the channel width has little effect on the detonation limit in the counterclockwise direction.

The critical tube width D/λ in the counterclockwise direction is basically unchanged, which is mainly because that as the detonation wave enters the annular channel from the straight pipe along the tangential direction, the outer wall's counterclockwise inclination angle (compared with the right horizontal direction) is close to 150°, the initial sparse effect is very strong, and the detonation wave is first completely decoupled, and then either continues to decay into a high-speed flame or re-initiate in some way. Thus the critical tube

width D/λ has no direct correlation with the width of the annular channel w. Conversely, in a clockwise direction, the detonation wave is less decoupled, and it is heavily influenced by reflections on the inner wall, so the critical tube width D/λ is directly related to the annular channel width w. As for the difference in critical tube width between the unstable and stable mixtures, the main reason may be that the stability difference between the three different mixtures used here is insignificant. According to Ng's work [17-18], the instability factor χ = 5.16 for C_2H_2+2.5O_2 at an initial pressure of 20 kPa and the instability factor χ = 3.24 for C_2H_2+2.5O_2+70% Ar at an initial pressure of 20 kPa. The instability factor of C_3H_8+5O_2 under the initial pressure of 20 kPa is as high as 16.6, and the instability factor of $2H_2$+O_2+40% Ar gas is as low as 0.91. Therefore, the slight difference in instability between the three mixtures explains the critical tube width trend in Fig.6.

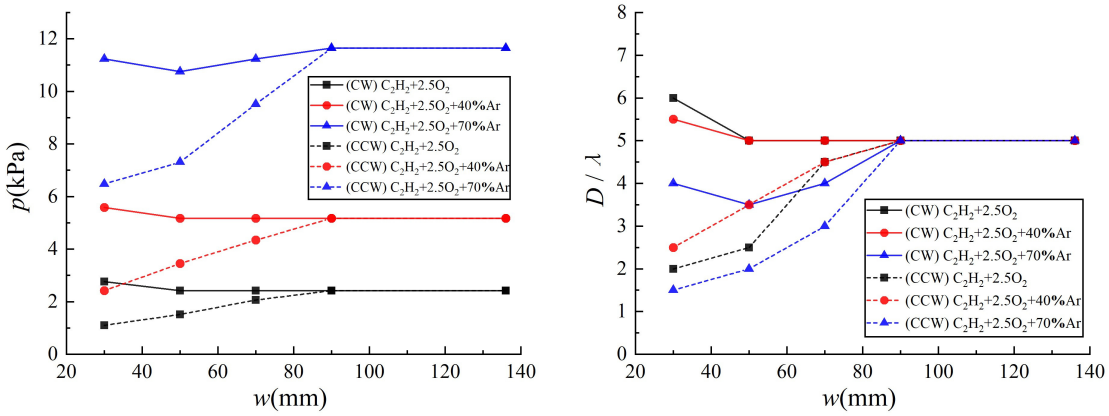

（a）Critical pressure （b）Critical pipe width

Fig.6 Detonation limits of different gases in annular channel

4 Conclusions

The CJ detonations diffract from the straight channel into the annular channel, propagating simultaneously in both clockwise and counterclockwise directions. The propagation mode can be divided into three modes: subcritical, critical and supercritical. However, the order in which these three modes appear in the clockwise and counterclockwise directions is not synchronized, and it is easier for detonation to fail in the counterclockwise direction. This is because in the clockwise direction, the detonation wave along the outer wall is first subjected to the sparse effect of diffraction, and then subjected to the compression of the reflection. However, in the counterclockwise direction, the detonation wave is always subjected to the compression of the outer wall. The study also found that re-detonation is achieved in two ways, one is through the reflection of the decoupled front on the inner wall and the subsequent transverse detonation wave, and the other is through the DDT process.

In the case of two-dimensional detonation diffraction, the critical tube width is 5λ for unstable gases and 13λ for stable gaeses. However, in this study, it was found that as the width of the annular channel became larger, despite of the concentration of argon, the critical tube width was close to that of the unstable detonation wave in the classical diffraction problem. If the width of the detonation channel is small, the detonation limit of the counterclockwise propagation direction is less than 5λ, and the detonation limit of the clockwise propagation direction is basically close to 5λ.

Acknowledgments

This work was supported by National Natural Science Foundation of China (No. 12072036).

References

[1] Hishida M, Fujiwara T, Wolanski P. (2019). Fundamentals of rotating detonations. Shock Waves, 19:1-10.

[2] Connolly-Boutin S, Joseph V, Ng HD, et al. (2021) Small-size rotating detonation engine: scaling and minimum mass flow rate. Shock Waves, 31: 665–674.

[3] Yi TH, Lou J, Turangan C, et al. (2011) Propulsive Performance of a Continuously Rotating Detonation Engine. J. Propul. Power. 2011, 27(1):171-181.

[4] Xia ZJ, Sheng ZH, Shen D W, et al. (2021). Numerical investigation of pre-detonator in rotating detonation engine. Int. J. Hydrogen Energ. 46: 31428-31438.

[5] Katta VR, Cho KY, Hoke JL, et al. (2019). Effect of increasing channel width on the structure of rotating detonation wave. Proc. Combust. Inst. 37(3): 3575-3583.

[6] Ding C, Wu Y, Xu G, Xia Y, Li Q, Weng C. (2022). Effects of the oxygen mass fraction on the wave propagation modes in a kerosene-fueled rotating detonation combustor. Acta Astronaut. 195:204-214,

[7] Li J, Ren H, Ning J. (2013). Numerical application of additive Runge-Kutta methods on detonation interaction with pipe bends. Int. J. Hydrogen Energ. 38(21): 9016-9027.

[8] Li J, Ning J, Zhao H, et al. (2015). Numerical investigation on the propagation mechanism of steady cellular detonations in curved channels. Chinese Physics Letters, 32(4): 048202.

[9] Thomas GO, Williams RL. (2002). Detonation interaction with wedges and bends. Shock Waves, 11(6): 481-492.

[11] Kudo Y, Nagura Y, Kasahara J, et al. (2011). Oblique detonation waves stabilized in rectangular-cross-section bent tubes. Proc. Combust. Inst. 33: 2319-2326.

[12] Nakayama H, Moriya T, Kasahara J, et al. (2012). Stable detonation wave propagation in rectangular-cross-section curved channels. Combust. Flame. 159: 859-869.

[13] Sugiyama Y, Nakayama Y, Matsuo A, et al. (2014). Numerical investigations on detonation propagation in a two-dimensional curved channel. Combust. Sci. Technol. 186: 1662-1679.

[14] Yuan XQ, Zhou J, Lin ZY, et al. (2016). Adaptive simulations of detonation propagation in 90-degree bent tubes. Int. J. Hydrogen Energ. 41: 18259-18272.

[15] Nagura Y, Kasahara J, Matsuo A. (2016). Multi-frame visualization for detonation wave diffraction. Shock Waves, 26(5): 645-656.

[16] Lee JHS. (2008). The Detonation Phenomenon. Cambridge: Cambridge University.

[17] Zhang B, Kamenskihs V, Ng HD, et al. (2011). Direct blast initiation of spherical gaseous detonations in highly argon diluted mixtures. Proc. Combust. Inst. 33: 2265-2271.

[18] Ng H D, Radulescu MI, Higgins A J, et al. (2005). Numerical investigation of the instability for one-dimensional Chapman-Jouguet detonations with chain-branching kinetics. Combust. Theor. Model. 9: 385-401.